Geomechanical behavior of relay ramps in a carbonate reservoir: Structural seismic interpretation impacts considerations on the flow pattern.

*Tatiana A. S. Oliveira (Petrobras), Thiago Falcão (Petrobras), Raquel Velloso (PUC-Rio), Flávia Falcão (Petrobras), Mario Neto (Petrobras).

This paper was prepared for presentation during the 16th International Congress of the Brazilian Geophysical Society held in Rio de Janeiro, Brazil, 19-22 August 2019.

Abstract

This study proposes to assess the geomechanical behavior of relay ramps during the development (injection and production) of a carbonate reservoir and the impacts of structural seismic interpretation on the flow pattern. Two 2D ramp models were built, with and without overlapping, and assigned to them two distinct materials, matrix and fault zone, with initial and boundary conditions definition. For each model two scenarios were tested: in the first one, where there is production and injection in the reservoir, which the response of the ramp geometry, in terms of pore pressure distribution and flow velocity, was evaluated. And in the second scenario, where there is only injection in the reservoir, the impacts on fluid flow were analyzed for two distinct hypotheses, one of sealing faults and the other of non-sealing faults. Two points of observation were chosen for evaluation. The results for the first scenario showed that the flow velocity tends to increase when it passes through the relay ramp and that these promotes a connection in the reservoir, stabilizing the pore pressure dissipation after a few years of production. In the second scenario, for the hypothesis of non-sealing faults, the observer points demonstrated that the geometry of the ramp did not influence the pore pressure dissipation, whereas, this influence was significant in the hypothesis of sealing faults, since the ramps act as preferential paths to the flow. This finding become more evident when the faults ramp geometry was modified. These changes demonstrated the importance of a coherent structural seismic interpretation that best represents the subsurface geological structures, once impacts the flow pattern.

Introduction

Normal fault segments are observed in Rift systems and crustal extension regions around the world (Coward et al., 1987; Davidson., 1994). Crider and Pollard (1998) state that the evolution of distensions promotes the development of the fault system and the mechanical interaction between them originate the relay ramps (figure 1). These structures formation during the development of normal faults is extremely common (Fossen and Rotevatn 2016). They are formed and destroyed continuously and occurs since centimeters scale on a map, up to hundreds of kilometers wide (Peacock et al., 2000; Soliva and Benedicto, 2004). The interaction between faults and the consequent formation of ramps depends on the density, distribution and arrangement of the fault system and the stress field involved (Fossen and Rotevatn 2016).

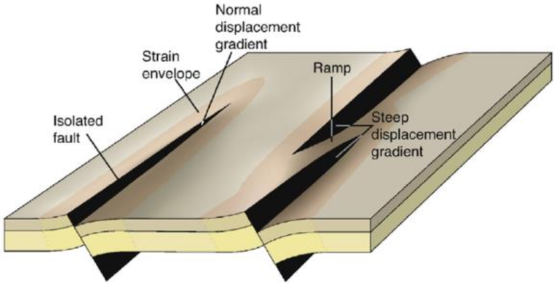

***Figure 1**: Relay ramp with normal faults connecting the hanging wall with footwall. Illustration shows how ramps are formed when two faults are close and their respective deformation envelopes overlap (right). An isolated fault is presented on the left side of the figure, Fossen and Rotevatn (2016).*

According to Fossen and Rotevatn (2016) the evolution of faults in a distensive system is due to one or the combination of one of the following mechanisms: growth and coalescence of the isolated faults segments or the reactivation of a deep crustal structure (figure 2). These models are considered end-members, which can explain the evolution of a fault system and occur naturally in the same region or Rift.

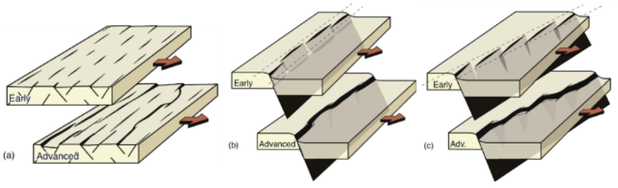

***Figure 2**: Evolution of faults in a distensive system. (a) Uniform extension generating an incipient fault system that evolves through the interconnection of smaller faults which become a single longer fault. (b) Basement controlling the extent and the generation of faults with standard in échelon in the sedimentary cover; that link up to non-planar large fault. (c) Variation of (b) where pre-existing faults are not orthogonal to the direction of extension. (Modified from Fossen and Rotevatn 2016).*

The evolution process of a faults system (growth, bonding, and amalgamation) is widely documented and relatively well understood (*e.g.* Peacock and Sanderson, 1991, Trudgill and Cartwright 1994, Cartwright et al., 1996, Cowie et al., Fossen et al., 2010, Fossen and Rotevatn 2016).

When two subparallel faults become close enough, they begin to interact and form the ramp. This is manifested by the curving of faults tips on the overlap zone, where a complex zone of subsidiary structures develops: faults, fractures and deformation bands (Fossen and Rotevatn 2016). When there is interaction of the faults and establishment of the relay ramp, it begins to deform internally and the ramp break can occur with distension processes continuity. The deformations depend essentially on the mechanical rock properties within the relay zone and the deformation ratio (Fossen et al., 1998).

Soft-linked relay ramps (without ramp break) are developed at the early stage of evolution of a distensive system. They form a zone where the deformation is transferred between two fault segments (figure 3a). The zone of intersection between the two faults is characterized by a higher topographically resultant region of the folding of the geological layers in the area (Peacock and Sanderson, 1991). As the distension evolves (figure 3b) a transfer fault is formed and the relay ramp is broken and initially separated into two coalescing segments, originating the hard-linked ramps and a continuous fault segment (figure 3c). This implies that soft-linked ramps have transition features in a progressive faulting process (Rotevatn et al., 2007).

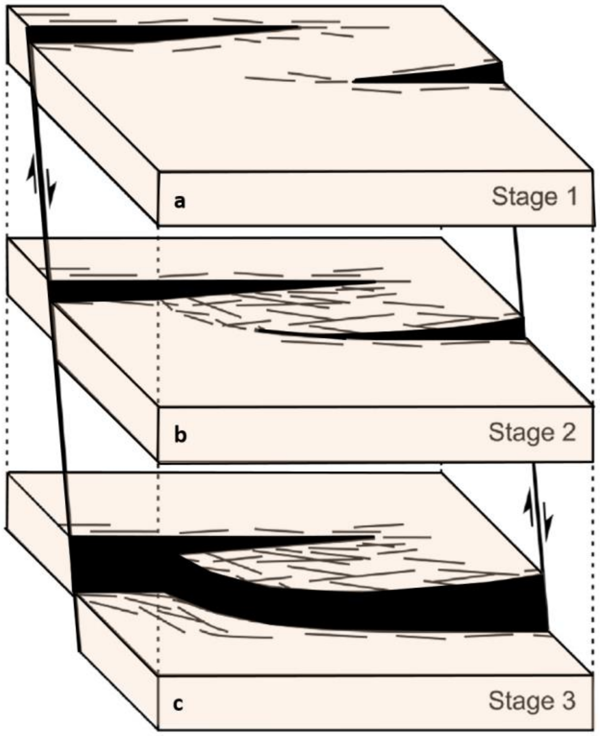

Figure 3*: Evolution of a distensive system: growth and connection of two fault segments through the formation of soft linked (stages 1 and 2) and hard-linked (stage 3) relay ramps. From stage 1 to 3 the development of a complex deformation zone is shown. In deeper levels a ramp can be hard-linked, whereas, at the shallower levels, it can be soft-linked ramp. (modified from Rotevatn et al 2007).*

Fossen and Rotevatn (2016) describe three end-members classes of ramp geometry that can be observed in field outcrops, interpreted seismic data, physical experiments and numerical models (figure 4): (1) ramp not broken (figure 4a) (2) evolution of only one fault tip (figure 4b), (3) evolution of the two faults tips (figure 4c) and (4) breach of the ramp without evolution of the fault tips (figure 4d).

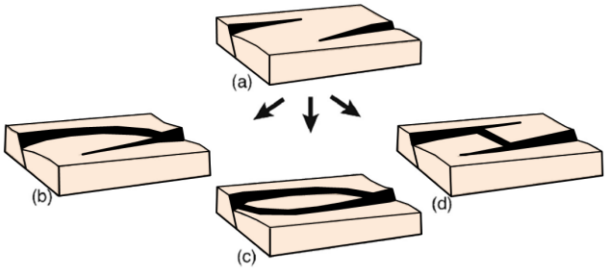

Figure 4*: Breaking patterns of relay ramps. (a) ramp not broken. (b) upper-ramp, evolution of only fault tip. (c) ramp with overlapping evolution of the both faults tips. (d) Mid-ramp, ramp breaks in half (Modified from Fossen and Rotevatn 2016).*

Relays ramps typically represent potential pathways for vertical fluids migration including hydrocarbons, CO2 and other hydrothermal solutions, metamorphic fluids, magma and groundwater (figure 5). They can act as conduits for fluid flow in the overlap zone between two sealing faults. The reason for this is the high structural complexity present in relay ramps with increasing numbers of faults and fractures and the wide range of orientations of these structures (e.g. Rowland and Sibson, 2004; Fossen et al., 1998).

Soft-linked relay ramps can increase permeability by the presence of fractures and faults, whereas in hard-linked ramps, due to the damage zone, permeability may be reduced (Rotevatn et al., 2007). However, in fractured carbonate reservoirs, it is demonstrated that hard-linked ramps can provide greater connectivity compared to soft-linked ramps. The reason is that in these rocks the development of the fracturing and permeability system is improving as the process of growth and connection of the faults evolves along the ramp becoming favorable to the flow until the total breakage of the relay ramp (Fossen e Rotevatn 2016).

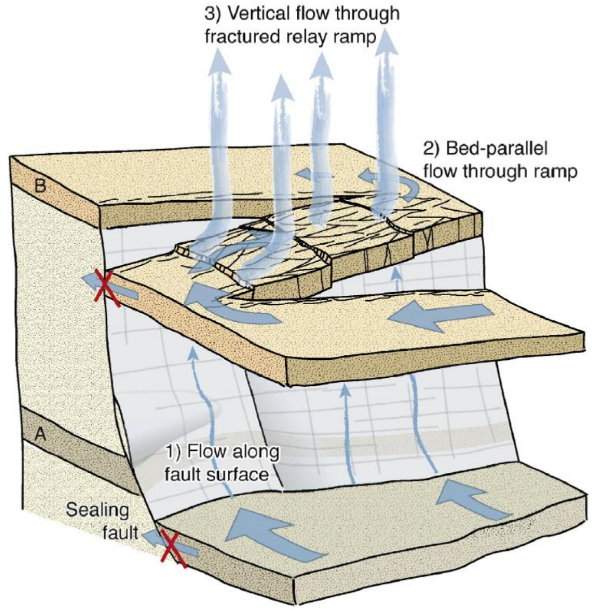

***Figure 5**: Fluid flow pattern through the relay ramp (layer (B)). The sealing fault can conduct the fluids in the vertical direction (1), but much more efficient is the flow through the fractured relay ramp (2). In reservoirs the relay ramps increase communication between the hangwall and footwall (2). Layer (A) does not present ramp geometry and is not associated with flow type 2 and 3, Fossen and Rotevatn (2016).*

Method

For this study two 2D models were built using the TECTOS @ PETROBRAS software, which is based on the finites elements method. Each model represents a stage of relay ramp evolution: with and without overlapping. For each model were assigned the materials that correspond to the reservoir rock (matrix) and deformed reservoir rock (fault zone). The positions of the injection and production wells were also chosen and the initial and boundary conditions were defined (figure 6).

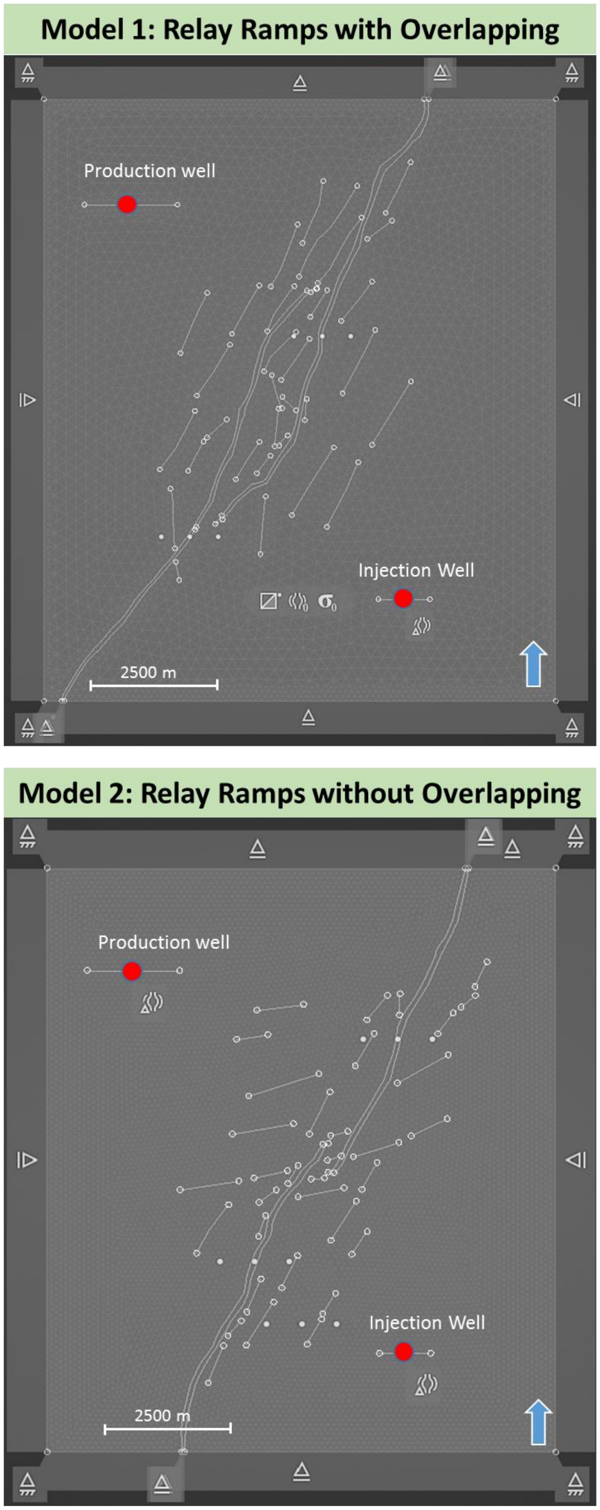

***Figure 6**: Two relay ramps 2D models. The first one, represents the relay ramps with overlapping and the second, without overlapping.*

The boundary conditions established for both models were restricted at x and y beyond the limits determined by the mesh area and the initial conditions of confining tension of 15 MPa in the x and y directions and initial pore pressure of 10 MPa for all mesh elements.

For each model, two scenarios were tested: in the first one, where there is production and injection in the reservoir, the response of the ramp geometry was evaluated for the pore pressure distribution and flow velocity during 30 years of simulation.

For the matrix and fault zone materials, values of density, porosity, permeability, Young's modulus, Poisson's coefficient, Biot's coefficient, with values related to carbonate rocks, close to those obtained in the Kiewiet, 2015 (Table 1).

For the injection and production wells, a differential of 10 MPa pore pressure was added, positive for the injection, considering increase of the pore pressure and negative for the production well, considering reduction of the pore pressure. The models were simulated for 30 years to evaluate the response of the ramp geometry regarding the pore pressure distribution and flow velocity.

Table 1: Scenario 1 geomechanical properties values for matrix and fault zone materials (adjusted from Kiewiet, 2015).

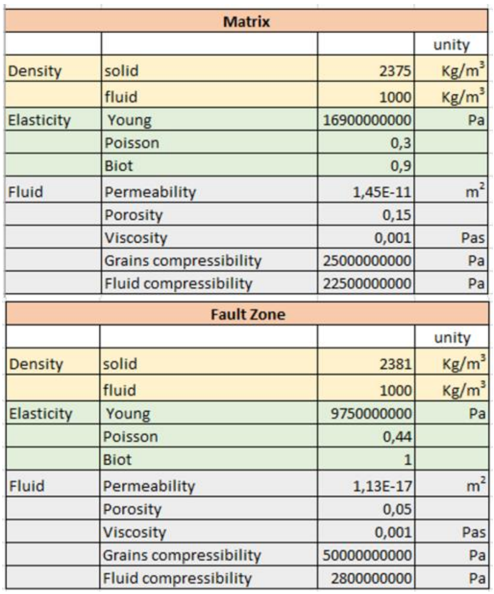

Matrix			
			unity
Density	solid	2375	Kg/m^3
	fluid	1000	Kg/m^3
Elasticity	Young	16900000000	Pa
	Poisson	0,3	
	Biot	0,9	
Fluid	Permeability	1,45E-11	m^2
	Porosity	0,15	
	Viscosity	0,001	Pas
	Grains compressibility	25000000000	Pa
	Fluid compressibility	22500000000	Pa

Fault Zone			
			unity
Density	solid	2381	Kg/m^3
	fluid	1000	Kg/m^3
Elasticity	Young	9750000000	Pa
	Poisson	0,44	
	Biot	1	
Fluid	Permeability	1,13E-17	m^2
	Porosity	0,05	
	Viscosity	0,001	Pas
	Grains compressibility	50000000000	Pa
	Fluid compressibility	2800000000	Pa

In the second scenario, where there is only injection in the reservoir, the impacts on fluid flow were analyzed for two distinct hypotheses: sealing and non-sealing faults. The geomechanical properties values for the matrix were maintained, as in scenario 1, and for the fault zones, were used those presented in table 2.

For the injection well, a positive differential pore pressure of 10 MPa was added and two observer points were chosen, one in the production well (A) and the other in the middle of the ramp (B). Their sensitivity was evaluated over the simulation time, due to the injection effect in the two hypotheses considered: sealing and non-sealing faults.

Also, in this second scenario it was analyzed the impacts on the flow pattern due to the structural seismic interpretation by modifying the faults configuration that constitute the relay ramp.

Table 2: Scenario 2 geomechanical properties values considering the hypotheses of sealing and non-sealing faults (adjusted from Kiewiet, 2015).

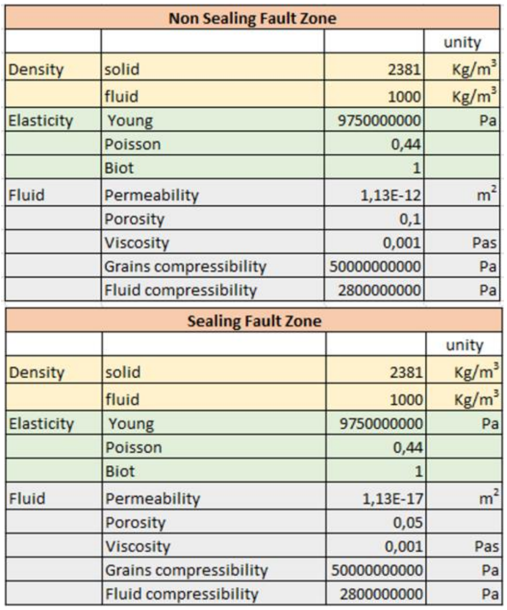

Non Sealing Fault Zone			
			unity
Density	solid	2381	Kg/m^3
	fluid	1000	Kg/m^3
Elasticity	Young	9750000000	Pa
	Poisson	0,44	
	Biot	1	
Fluid	Permeability	1,13E-12	m^2
	Porosity	0,1	
	Viscosity	0,001	Pas
	Grains compressibility	50000000000	Pa
	Fluid compressibility	2800000000	Pa

Sealing Fault Zone			
			unity
Density	solid	2381	Kg/m^3
	fluid	1000	Kg/m^3
Elasticity	Young	9750000000	Pa
	Poisson	0,44	
	Biot	1	
Fluid	Permeability	1,13E-17	m^2
	Porosity	0,05	
	Viscosity	0,001	Pas
	Grains compressibility	50000000000	Pa
	Fluid compressibility	2800000000	Pa

Results

The results of the first scenario showed that the flow velocity tends to increase when passing through the relay ramp in the two models tested. It was also observed that the ramps promote a connection between the hanging wall and footwall from the fault reservoir, stabilizing the pore pressure after a few years of production (figure 7).

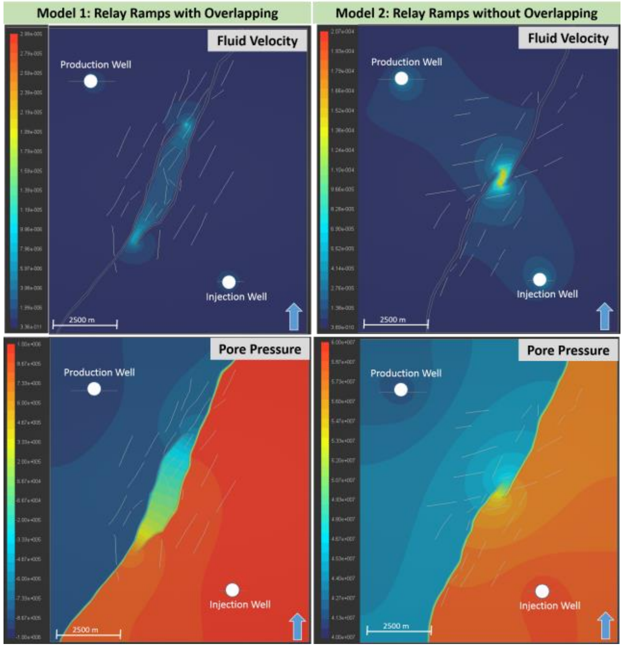

***Figure 7**: Scenario 1 maps for models 1 and 2 after 30 years of simulation. At the top, the fluid velocity maps and at the lower, the pore pressure maps.*

As for the ramp's geometry, it can be observed that in the ramps without overlapping, the flow velocity is much larger than those with the overlapping ramps. And also, that the pore pressures dissipate more easily on ramps without overlapping, showing that in a scenario of reservoirs production and injection with sealing faults characteristics, overlapping ramps tends to compartmentalize the reservoir more than in ramps without overlapping.

In scenario 2, for the hypothesis of non-sealing faults, the observer points demonstrated that the ramp geometry did not influence the pore pressure dissipation, that is, it didn't modify the flow pattern. The graphs from the observer points (A) and (B) confirm that the pore pressure dissipation stabilizes early in the first years of simulation (figure 8).

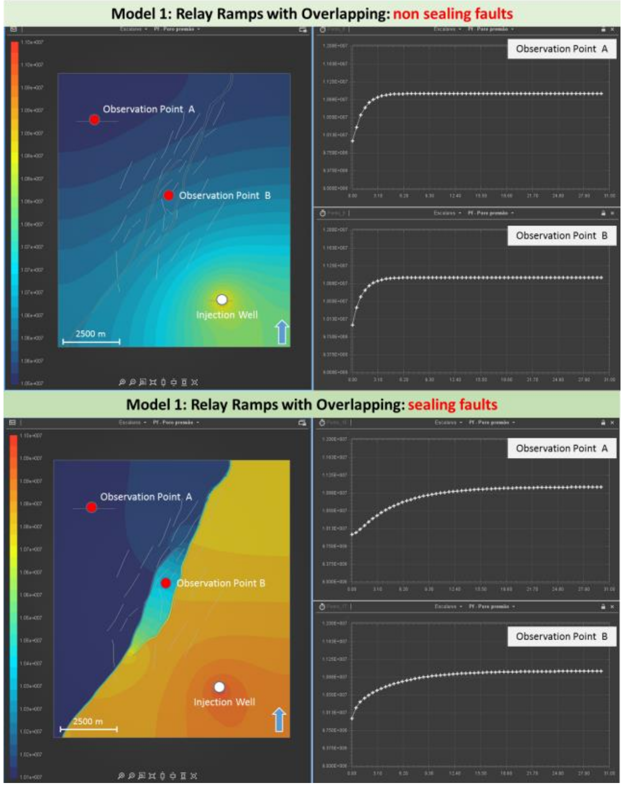

Figure 8*: Scenario 2 with relay ramps with overlapping, for the hypotheses of sealing and non-sealing faults. The graphs to the right (pore pressure versus time), present the results of these simulations in observer points (A) and (B).*

On the other hand, in case of sealing faults, the influence of the ramp geometry was significant, since the ramps act as preferential paths to the flow, making the flow pattern tortuous. The graph from the observer point (A) demonstrated that the pore pressure stabilization occurred in a time four times greater than the hypothesis with non-sealing faults, as well as to the observer point (B), in which the pore pressure stabilization occurred in a time three times greater than the hypothesis with non-sealing faults (figure 8).

For scenario 2, considering a change in the structural seismic interpretation of the ramp geometry, where one fault tip connects with the other fault and forms a single fault segment and when repeating the simulation, considering the assumptions of sealing and non-sealing faults, it is possible to evaluate the impact that the change at the structural seismic interpretation caused in the flow pattern (figure 9).

In the first case, in the hypothesis of non-sealing faults, it is noted that the ramp geometry did not influenced the pore pressure propagation, that is, it did not modify the flow distribution pattern as observed with the open ramp. However, when considering the hypothesis of sealing faults, the change in flow pattern is significant. The graph from the observer point (A) almost does not change its pore pressure values, which means that the reservoir is compartmentalized, while the graph from the observer point (B) stabilizes the pore pressure dissipation, since it is connected to the injection well by the relay ramp (figure 9).

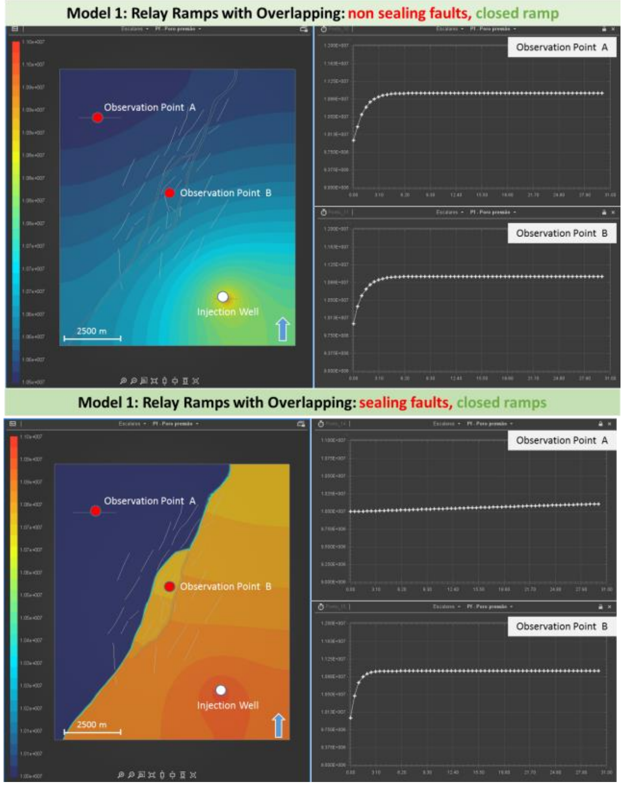

Figure 9*: Scenario 2 with relay ramps with faults connected (closed ramp) for the hypotheses of sealing and non-sealing faults. The graphs to the right (pore pressure versus time), present the results of these simulations in observer points (A) and (B).*

Conclusions

Relay ramps impacts the flow pattern when their faults have a sealing character.

The different relay ramps geometries, with and without overlapping, influence the flow pattern, and those with overlapping cause a more significant influence in the pore pressure dissipation than those without overlapping.

All the scenarios tested demonstrated the importance of a coherent and representative structural seismic interpretation of the subsurface geological structures for the flow simulation, since changes in the geometry of the ramps, closed or open, considering the same geomechanical properties for the faults, influence the flow pattern. This finding becomes more relevant in the absence of dynamic reservoir data.

Future studies will portray in more detail the fault zone elements (damage zone and core), and the adoption of a material representing the existing deformation in the relay ramp area. Therefore, better understanding the geomechanical behavior of the relay ramps during the development of the reservoir, in terms of flow distribution and faults reactivation.

Acknowledgments

We would like to thanks Petrobras and PUC-RIO for the opportunity to develop this study, the geophysicist Alexandre Maul for the review and all those who contributed with the ideas and the results interpretation.

References

Cartwright, J.A., Mansfield, C.S., Trudgill, B.D., 1996. Fault growth by segment linkage. In: Buchanan, P.C., Nieuwland, D.A. (Eds.), Modern Developments in Structural Interpretations, Geological Society Special Publications, vol. 99, pp. 163 e 177.

Coward, M.P., Dewey J.F., Hancock P.L., 1987, Continental extensional tectonics Geol. Soc. Spec. Publ., 28, 637 pp.

Crider, J.G., Pollard, D.D., 1998. Fault linkage: three-dimensional mechanical interaction between echelon normal faults. J. Geophys. Res. 103, 675–692.

Cowie, P.A., Underhill, J.R., Behn, M.D., Lin, J., Gill, C.E., 2005. Spatio-temporal evolution of strain accumulation derived from multi-scale observations of Late Jurassic rifting in the northern North Sea: a critical test of models for lithospheric extension. Earth and Planetary Science Letters 234, 401 e 419.

Davidson, I., 1994. Linked fault systems extensional, strike-slip & contractional, in Continental Deformation edited by P.L. Hancock. Pergamon, Tarrytown, N.Y. pp. 121-142,

Fossen, H., Hesthammer, J., 1998. Structural geology of the Gullfaks Field, northern North Sea. Geol. Soc. Lond. Spec. Publ. 127, 231–261.

Fossen, H., Rotevatn, A., 2016. Fault linkage and relay structures in extensional settings – a review. Earth Science Reviews Publ. 154, 14-28.

Peacock, D. C. P., Price S. P., Pickles C. S., 2000. The world’s biggest relay ramp: HoldWith Hope, NE Greenland: Journal of Structural Geology v. 22, p. 843–850.

Peacock, D.C.P., Sanderson, D.J., 1991. Displacements, segment linkage and relay ramps in normal fault zones. Journal of Structural Geology 13, 721 e 733.

Peacock, D.C.P., Sanderson, D.J., 1994. Geometry and development of relay ramps in normal fault systems. AAPG Bulletin 78, 147 e 165.

Kiewiet, M. C. D. N., 2015. Comportamento Hidromecânico de Zona de Falha em Travertino: Estudo experimental e Numérico sobre o impacto da Reativação estrutural na produção de reservatórios. Instituto de Geociências, UFRJ. 652 (Doutorado).

Rotevatn, A., Fossen, H., Hesthammer, J., Howell, J.A., 2007. Are relay ramps conduit for fluid flow? Structural analysis of a relay ramp in Arches National Park, Utah. In Lonergan, L., Jolly, R.J.H., Sanderson, D.J., Rawnsley, K. (Eds.), Fractured Reservoirs, Geological Society Special Publications, vol.270, pp. 55-71.

Rowland, J.V., Sibson, R.H., 2004. Structural controls on hydrothermal flow in a segmented rift system, Taupo Volcanic Zone, New Zealand. Geofluids 4, 259–283.

Soliva, R., A. Benedicto, 2004. A linkage criterion for segmented normal faults: Journal of Structural Geology, v. 26, p. 2251–2267.

Trudgill, B.D., Cartwright, J.A., 1994. Relay ramp forms and normal fault linkages, Canyonlands National Park, Utah. GSA Bulletin 106, 1143e1157.